Project 2438 | April 2025

SJSU SAN JOSÉ STATE UNIVERSITY

MTI MINETA TRANSPORTATION INSTITUTE

Evaluation of Long-Term Performance of Transportation Earthworks Prone to Weather-Driven Deterioration Under Changing Climate

Amr M. Morsy, PhD, PE   Emma Varela

California State University Transportation Consortium

CALIFORNIA STATE UNIVERSITY LONG BEACH

MINETA TRANSPORTATION INSTITUTE

Founded in 1991, the Mineta Transportation Institute (MTI), an organized research and training unit in partnership with the Lucas College and Graduate School of Business at San José State University (SJSU), increases mobility for all by improving the safety, efficiency, accessibility, and convenience of our nation's transportation system. Through research, education, workforce development, and technology transfer, we help create a connected world. MTI leads the Mineta Consortium for Emerging, Efficient, and Safe Transportation (MCEEST) funded by the U.S. Department of Transportation, the California State University Transportation Consortium (CSUTC) funded by the State of California through Senate Bill 1 and the Climate Change and Extreme Events Training and Research (CCEETR) Program funded by the Federal Railroad Administration. MTI focuses on three primary responsibilities:

Research

MTI conducts multi-disciplinary research focused on surface transportation that contributes to effective decision making. Research areas include: active transportation; planning and policy; security and counterterrorism; sustainable transportation and land use; transit and passenger rail; transportation engineering; transportation finance; transportation technology; and workforce and labor. MTI research publications undergo expert peer review to ensure the quality of the research.

Education and Workforce Development

To ensure the efficient movement of people and goods, we must prepare the next generation of skilled transportation professionals who can lead a thriving, forward-thinking transportation industry for a more connected world. To help achieve this, MTI sponsors a suite of workforce development and education opportunities. The Institute supports educational programs offered by the Lucas Graduate School of Business: a Master of Science in Transportation Management, plus graduate certificates that include High-Speed and Intercity Rail Management and Transportation Security Management. These flexible programs offer live online classes so that working transportation professionals can pursue an advanced degree regardless of their location.

Information and Technology Transfer

MTI utilizes a diverse array of dissemination methods and media to ensure research results reach those responsible for managing change. These methods include publication, seminars, workshops, websites, social media, webinars, and other technology transfer mechanisms. Additionally, MTI promotes the availability of completed research to professional organizations and works to integrate the research findings into the graduate education program. MTI's extensive collection of transportation-related publications is integrated into San José State University's world-class Martin Luther King, Jr. Library.

Report 25-07

Evaluation of Long-Term Performance of Transportation Earthworks Prone to Weather-Driven Deterioration Under Changing Climate

Amr M. Morsy, PhD, PE

Emma Varela

April 2025

A publication of the
Mineta Transportation Institute
Created by Congress in 1991

College of Business
San José State University
San José, CA 95192-0219

TECHNICAL REPORT DOCUMENTATION PAGE

1. Report No.	2. Government Accession No.	3. Recipient's Catalog No.
25-07		

4. Title and Subtitle	5. Report Date
Evaluation of Long-Term Performance of Transportation Earthworks Prone to Weather-Driven Deterioration Under Changing Climate	April 2025
	6. Performing Organization Code
7. Authors	**8. Performing Organization Report**
Amr Morsy: 0000-0002-9335-7847 Emma Varela: 0009-0001-9931-3503	CA-MTI-2438
9. Performing Organization Name and Address	**10. Work Unit No.**
Mineta Transportation Institute College of Business San José State University San José, CA 95192-0219	**11. Contract or Grant No.** SB1-SJAUX_2023-26
12. Sponsoring Agency Name and Address	**13. Type of Report and Period Covered**
State of California SB1 2017/2018 Trustees of the California State University Sponsored Programs Administration 401 Golden Shore, 5th Floor Long Beach, CA 90802	**14. Sponsoring Agency Code**

15. Supplemental Notes
10.31979/mti.2025.2438

16. Abstract
Embankments are key transportation infrastructure features providing essential support for long, linear stretches of transportation infrastructure, including highways and railways, in California and globally. Clay embankments are susceptible to weather-related deterioration processes that can gradually compromise their stability and, in some cases, lead to unexpected failures. Climate change, along with the associated shifts in weather patterns, is projected to adversely impact weather-related deterioration processes, leading to exacerbated failures and/or shorter service life. This study evaluated the impact of climate change on the rate of weather-driven deterioration of embankments in two locations in California: Los Angeles and Sacramento. Specifically, a multi-phase hydromechanical geotechnical model was developed for an exemplar clay embankment. The model is capable of simulating long-term performance of an embankment subject to a climate-controlled flux boundary. The model was used to perform numerical simulations where temperature and rainfall levels were adjusted to reflect four possible future climate change scenarios: Case (1) no average temperature or average precipitation changes; Case (2) +3°C average temperature change and –12.5% average precipitation change; Case (3) +3°C average temperature change and no average precipitation change; and Case (4) +3°C average temperature change and +12.5% average precipitation change. Performance indicators were obtained from the numerical simulations to compare the effect of climate change in Los Angeles and Sacramento. It was concluded that climate change is generally projected to adversely affect the long-term performance of clay embankments, which can put critical transportation infrastructure and the communities that depend on it at risk.

17. Key Words	18. Distribution Statement
Embankments, earthwork, climate change, weathering, deterioration by environmental action.	No restrictions. This document is available to the public through The National Technical Information Service, Springfield, VA 22161.

19. Security Classif. (of this report)	20. Security Classif. (of this page)	21. No. of Pages	22. Price
Unclassified	Unclassified	50	

Form DOT F 1700.7 (8-72)

DOI: 10.31979/mti.2025.2438

Mineta Transportation Institute
College of Business
San José State University
San José, CA 95192-0219
Tel: (408) 924-7560
Fax: (408) 924-7565
Email: mineta-institute@sjsu.edu

transweb.sjsu.edu/research/2438

Acknowledgments

This study was supported by the California State University Transportation Consortium (CSUTC) through its Transportation Research & Training (TRANSPORT) grant funded by California Senate Bill 1 (SB 1): The Road Repair and Accountability Act of 2017. The opinions presented in this report are those of the authors and are not necessarily those of the CSUTC. The report cover photo belongs to ©Puckillustrations/AdobeStock.

CONTENTS

LIST OF FIGURES

LIST OF TABLES

Executive Summary

Earthworks are a key feature of the transportation network, supporting long, linear stretches of highways and railways not only in California but also globally. Transportation embankments are susceptible to weather-related deterioration processes that can gradually compromise their stability and, in some cases, lead to unexpected failures, particularly in aging infrastructure. California's recent rainy season of 2017, following a five-year drought, has caused severe flooding, landslides, and coastal erosion, totalling over $1 billion in highway damages for the California Department of Transportation (Caltrans). Given that California plays a pivotal role as a major provider of goods and services to the broader United States, any disruption in its transportation system could have calamitous repercussions for the entire nation, as per California's Fourth Climate Change Assessment report.

According to a recent NCHRP survey on surficial embankment failures, California is responsible for approximately 15,092 road miles, 40% of which are estimated to be susceptible to surficial failures. Approximately 80% of embankment failures in California embankments are considered surficial (less than 3 m deep) and 20% are considered deep-seated (larger than 3 m deep). Surficial embankment failures commonly occur following severe weather events or a pattern of events, a relationship that has also been observed in California. The approximate service life at which a surficial failure triggers in embankments in California is 20 to 40 years, assuming they were designed and constructed appropriately.

Weather-driven deterioration involves a complex suite of mechanisms that are insidious to the behavior of embankment fill over time, including seasonal variations in near-surface soil moisture and pore pressure. These complex processes introduce considerable uncertainty regarding the rate of deterioration and the current condition of existing earthworks assets. Further, climate change, along with the associated shifts in weather patterns, is projected to adversely impact the behavior of transportation earthworks and exacerbate their weather-driven deterioration.

This study evaluated the impact of climate change on the rate of weather-driven deterioration of embankments in two locations in Los Angeles and Sacramento. A multi-phase hydromechanical geotechnical model was developed for an exemplar clay embankment to simulate the long-term performance of an embankment subject to a climate-controlled flux boundary. The model was used to perform numerical simulations with various climate perturbed parameter ensembles of four future climate scenarios:

- Case (1) no average temperature or average precipitation changes.
- Case (2) +3°C average temperature change and –12.5% average precipitation change.

- Case (3) +3°C average temperature change and no average precipitation change.
- Case (4) +3°C average temperature change and +12.5% average precipitation change.

This study provided a few insights into the effect of climate change on clay embankments. Notably, the results of this study indicated that rate of increase in irrecoverable vertical displacements reduced over time as soil swelling reaches its potential, whereas the increase in irrecoverable outward displacement persists over time. Swelling-induced shallow slides are likely triggered at this condition. This is likely to occur in high plasticity clays after 70 years in Los Angeles climate and after 45 years in Sacramento climate. Existing embankments constructed from high plasticity clays that are older than these limits and whose failure consequences are high may require risk mitigation strategies (e.g., monitoring).

Performance indicators were obtained from the numerical simulations to compare the effect of climate change in Los Angeles and Sacramento. Overall, it was concluded that climate change is generally projected to adversely affect the long-term performance of clay embankments. This effect varies significantly based on the climate zone. Long-term performance predictions for embankments other than the emblematic embankment studied herein or constructed in climate types other than those studied herein can be obtained by running additional simulations using the numerical model presented in this study. Tentatively, the long-term performance of embankments comparable to the emblematic embankment studied herein and at other climate zones may be approximated by adjusting the results predicted at the exemplar locations studied herein using relevant climate zone characteristic parameters, such as the ratio of the average annual potential evapotranspiration to the average annual precipitation (PET/P).

It is evident that numerical models that consider the influence of weather-related factors on the degradation and potential failure of earthworks, such as the one presented in this study, can provide insights into the long-term behavior of transportation infrastructure that is prone to weather-driven deterioration. Such insights can be of significant value to infrastructure asset management. Prediction of potential failures allows infrastructure stakeholders to plan proactive intervention (e.g., maintenance, repair, rehabilitation), optimize budget allocation, and reduce overall maintenance costs. This approach can significantly increase the longevity of assets, leading to cost savings over the long term.

1. Introduction and Background

Earthworks play a vital role in the transportation network, providing essential support for long-linear stretches of highways and railways not only in California but also globally. However, these earthworks are susceptible to insidious weather-driven deterioration processes that can lead to unexpected failures, particularly in aging earthworks, including cuttings and embankments (Stirling et al. 2021; Postill et al. 2021; Morsy et al. 2023a; Helm et al. 2024). California's recent rainy season of 2017, following a five-year drought, has caused severe flooding, landslides, and coastal erosion, totalling over $1 billion in highway damages for Caltrans (Caltrans 2018). Given that California plays a pivotal role as a major provider of goods and services to the broader United States, any disruption in its transportation system could have calamitous repercussions for the entire nation (Bedsworth et al. 2018).

1.1 Overview of the Problem

According to a survey conducted by Beckstrand and Bunn (2024) as part of an NCHRP synthesis on surficial (i.e., shallow) embankment failures, California is responsible for approximately 15,092 road miles, 40% of which are estimated to be susceptible to surficial failures. Approximately 80% of embankment failures in California embankments are considered surficial (less than 3 m deep) and 20% are considered deep-seated (larger than 3 m deep). Surficial embankment failures commonly occur following severe weather events, a relationship that has also been observed in California. The approximate service life before a surficial failure triggers in embankments in California is 20 to 40 years, assuming the embankments were designed and constructed appropriately.

The performance of infrastructure assets supported by soil slopes is affected by time-dependent deterioration processes of soils. It is evident that weather-driven deterioration mechanisms contribute significantly to the overall deterioration of earth infrastructure assets that can lead to progressive failures, especially those of compacted clay slopes (e.g., Templeton et al. 1984; Vaughan et al. 2004; Nyambayo et al. 2004; Rouainia et al. 2009; Nyambayo and Potts 2010; Kovacevic et al. 2013; Morsy et al. 2023a). Weather-driven deterioration involves a complex suite of mechanisms that gradually alter the hydromechanical properties of soils over time, including seasonal variations in pore pressure due to changing weather and climate (Stirling et al. 2021). Further, climate change, along with the associated shifts in weather patterns, is anticipated to manifest both nationally and globally (Masson-Delmotte 2021).

These transformations are expected to exert adverse impacts on the hydromechanical behavior of geotechnical infrastructure, including earthworks, and on the rate of their weather-driven deterioration (Helm et al. 2024). It is notable that the California Department of Transportation (Caltrans) have set plans for analyzing the effects of climate change on the state's transportation infrastructure in order to strengthen and protect it from damage, which is in compliance with the state efforts to "translate the state of climate science into useful information for action" across the state (Caltrans 2018) as per the California's Fourth Climate Change Assessment report (Bedsworth et al. 2018).

Weather-driven deterioration models for earthworks are essential for understanding how climate and environmental conditions can impact the stability and longevity of the infrastructure assets supported by these earthworks. Generally, deterioration models rely on real-time or historical field data that can inform asset management decision-making. However, problems such as weather-driven deterioration of clay embankments can be quite challenging due to the scarcity of field data and their correlation to imminent failure. Accordingly, enhanced capabilities are required to forecast future performance and the remaining service life of aging infrastructure using robust and reliable modeling approaches that can account for weather-driven deterioration under a range of climate projections. According to the California Transportation Asset Management Plan (TAMP 2022), opportunities identified for future improvements in transportation asset management include "enhancing asset modeling capabilities."

1.2 Research Objectives

Using numerical modeling, this study aimed to assess the impact of climate change on the rate of weather-driven deterioration of earthworks in California. The specific objectives of this study include (1) the development of multi-phase hydromechanical numerical models to simulate long-term performance of transportation earthworks, (2) the generation of perturbed climate suites, and (3) the assessment of long-term performance of earthworks under various climate change scenarios.

1.3 Report Organization

This report consists of the following sections:

- Section 1. Introduction and Background. This section presents the overview of the problem, research questions, research objectives, and report organization.

- Section 2. Numerical Model. This section presents the development of the numerical model.

- Section 3. Perturbed Climate. This section documents the perturbed climate suites generated for California climate.

- Section 4. Parametric Study. This section presents and discusses the results of a parametric study of long-term performance of earthworks under various climate change scenarios.

- Section 5. Summary and Recommendations. This section summarizes the study documented in this report and provides practical recommendations based on its findings.

2. Numerical Model

This study used a numerical modeling approach that was previously developed by Morsy et al. (2023a) specifically for simulating the weather-driven deterioration of earthworks. This modeling approach has undergone validation, demonstrating its effectiveness in capturing the long-term hydromechanical behavior of earthworks (Morsy et al. 2023a, 2023b). The validation process involved a comprehensive study using a full-scale research embankment equipped with 9 years of monitoring data, including parameters such as soil moisture, matric suction, and settlement. Additionally, the modeling approach was successfully validated to predict the service life (i.e., time to failure) for 34 well-documented failure case histories (Morsy and Helm 2024a, 2024b).

2.1 Model Description

The embankment numerical model was developed using FLAC (Fast Lagrangian Analysis of Continua) software v8.1. This software was used to run hydromechanical simulations to study long-term behavior of the modeled embankment under various climate scenarios. The model was developed using 0.5 m $\times$ 0.5 m mesh zones, as shown in Figure 1. The mesh zone size was chosen as twice the typical construction lift thickness (2 $\times$ 0.25 m) to facilitate the modeling of the construction stages. To model the staged construction, the mesh layout was selected with horizontal mesh zone layers. A detailed description of the model mesh and its development is provided in Morsy et al. (2023a). Subroutines were developed to automatically create the models with various geometries with slope heights that are multiples of 0.5 m (Morsy 2024).

2.2 Boundary Conditions

The bottom boundary was constrained in both the horizontal and vertical directions. The lateral boundaries were constrained from displacement in the horizontal direction and were free to displace in the vertical direction. The initial groundwater elevation was specified at a relatively large depth below the original ground surface (i.e., the base of the embankment) for all models. This assumption can be justified since the average groundwater depth in the study areas is generally deep below ground surface as per the groundwater data available through California Groundwater Live by California Department of Water Resources (CA DWR 2024). A transient climate boundary was defined at the surface of the model to simulate soil-atmosphere interaction. The climate boundary calculates the daily surface net flux as the difference between precipitation and actual evapotranspiration. A detailed description of the model climate boundary is provided in Morsy et al. (2023a).

2.3 Initial Conditions

The effective vertical stresses were initialized in the foundation soil using the effective overburden stress and the effective horizontal stresses were initialized using an at-rest coefficient, K_o, of 1.0. Embankment layers were activated in the model incrementally to simulate embankment construction. A detailed description of model initialization and construction simulation is provided in Morsy et al. (2023a).

Figure 1. Finite-Difference Mesh Used to Model One Half of a Symmetrical Embankment

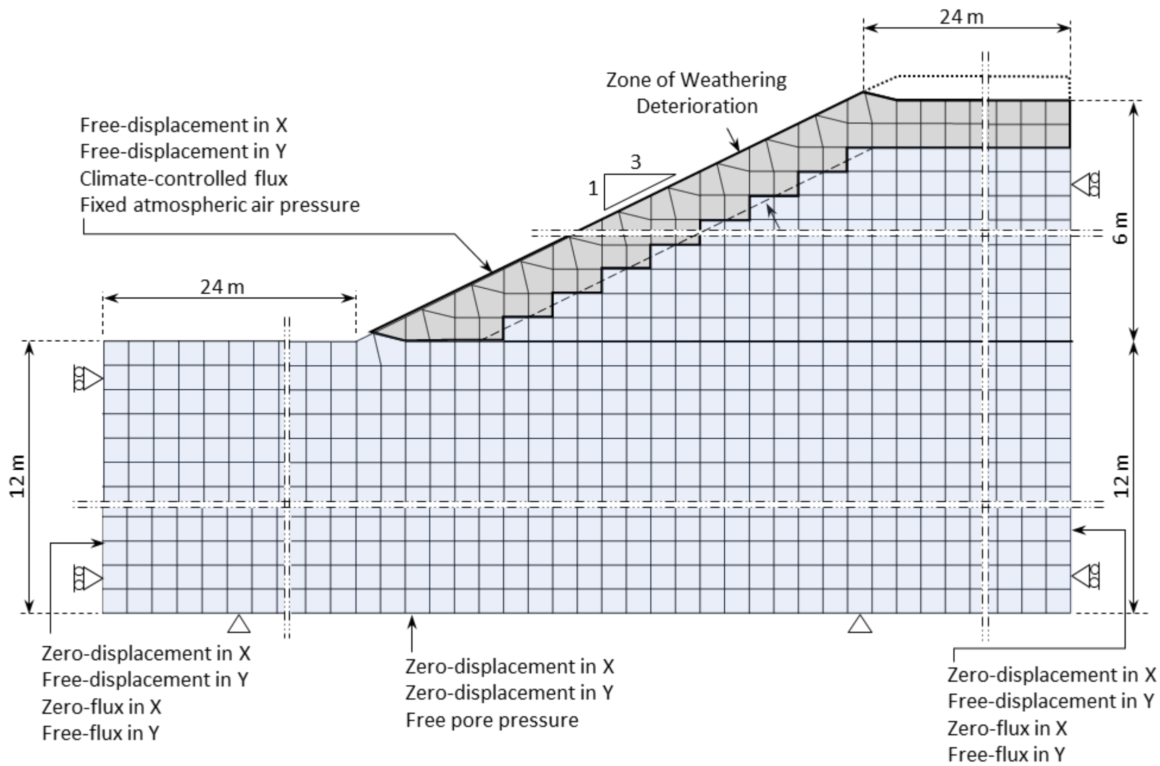

Adapted from Morsy and Helm 2024a.

2.4 Mechanical Behavior

The mechanical behavior of the fill materials was modeled using a multi-stage Mohr-Coulomb model with strain softening to simulate the change in mechanical behavior of clays over time. Mohr-Coulomb parameters (cohesion intercept, c, angle of internal resistance, ϕ, , and angle of dilation, ψ) varied with accumulated ratcheting plastic strain and with seasonal wet-dry cycles in the near surface. A detailed description of the model is provided in Morsy and Helm (2024a).

Young's modulus, E, of the soil was defined as a function in mean effective stress, σ'_m, as suggested by Kulhawy et al. (1969):

$$E = E_o p_o \left(\frac{\sigma'_m}{p_o}\right)^{m_E}, \ \frac{\sigma'_m}{p_o} \geq 0.1 \qquad (1)$$

where E_o is Young's modulus at 1 atm, p_o is the atmospheric pressure (1 atm), and m_E is the Young's modulus stress exponent. Poisson's ratio, υ, of the soil was defined as a function in mean effective stress, σ_m' , as suggested by Kulhawy et al. (1969):

$$\upsilon = \upsilon_o - \ln\left(\frac{\sigma_m'}{p_o}\right)^{m_\upsilon}, \ \frac{\sigma_m'}{p_o} \geq 0.1 \qquad (2)$$

where υ_o is Poisson's ratio at 1 atm, p_o is the atmospheric pressure, and m_υ is the Poisson's ratio stress exponent. Mean effective normal stresses, σ_m', were modeled based on Bishop's generalized effective stress (Bishop 1959):

$$\sigma_m' = \sigma_m - u_a + \chi(u_a - u_w) \qquad (3)$$

where σ_m is the mean total normal stress, u_a is the pore-air pressure, u_w is the pore-water pressure, and χ is Bishop's effective stress parameter, and which be approximated to the degree of water saturation, S_w.

2.5 Hydraulic Behavior

Fluid transport in the finite-difference code used in this study is described by Darcy's law (Itasca 2019). The soil-water retention curve was developed based on field measurements and were represented using the van Genuchten (1980) fitting model for both the embankment fill and the foundation soil, as follows:

$$\psi_m = \psi_{m,o}\left({S_e}^{-1/a_{vg}} - 1\right)^{1-a_{vg}} \qquad (4)$$

where ψ_m is the matric suction, $\psi_{m,o}$ is a fitting parameter related to the air-entry matric suction; a_{vg} is a fitting parameter; and S_e is the effective saturation, which can be written as $S_e = \frac{S_w - S_{w,r}}{1 - S_{w,r}}$, where $S_{w,r}$ is the residual degree of water saturation. The model treats pore fluids as two immiscible fluids whose volumes make up the total void volume. Accordingly, the sum of the degree of air saturation, S_g, and the degree of water saturation is always equal to unity, $S_g + S_w = 1$.

The hydraulic conductivity function was correlated to the soil-water retention curve using the van (Mualem 1976; van Genuchten 1980) as $k_w = \kappa_{r,w}\ k_{w,sat}$, where k_w is the hydraulic conductivity, $k_{w,sat}$ is k_w at $S_w = 1$, and $\kappa_{r,w}$ is the relative hydraulic conductivity, which can be expressed as follows:

$$\kappa_{r,w} = {S_e}^{0.5}\left[1 - \left(1 - {S_e}^{1/a_{vg}}\right)^{a_{vg}}\right]^2 \qquad (5)$$

The air conductivity function was correlated to the hydraulic conductivity function (Parker et al. 1987) as $k_g = \kappa_{r,g}\ k_{g,sat}$, where k_g is the air conductivity, and $k_{g,sat}$ is k_g at $S_w = 1$, which was correlated to the saturated hydraulic conductivity and the ratio of water dynamic viscosity to air dynamic viscosity, μ_r (typically 55), as $k_{g,sat} = \gamma_g \ \mu_r \ k_{w,sat}$, and $\kappa_{r,g}$ is the relative air conductivity, which can be expressed as follows:

$$\kappa_{r,g} = (1 - S_e)^{0.5}\left(1 - {S_e}^{1/a_{vg}}\right)^{2a_{vg}} \tag{6}$$

The saturated hydraulic conductivity, $k_{w,sat}$, was correlated to the void ratio, e, according to the empirical formula proposed by Samarasinghe et al. (1982) as $k_{w,sat} = C\left(\frac{e^l}{1+e}\right)$, where C and l are empirical parameters that depend on the clay mineralogy.

2.6 Embankment Parameters

According to a survey conducted by Beckstrand and Bunn (2024) as part of an NCHRP synthesis on surficial (i.e., shallow) embankment failures, California does not maintain inventories of embankment attributes (height, length, side-slope angles, material, year of construction). Accordingly, ranges of embankment attributes were derived for a typical high-plasticity clay fill, which is the most sensitive fill to weather-driven deterioration. Table 1 summarizes the parameters of the mechanical and hydraulic models adopted for the emblematic embankment modeled in this study. Figures 2a and 2b show the variation of the angle of internal resistance and cohesion intercept with plastic strain respectively based on the shear strength model adopted in this study. Note that the cohesion intercept peak was allowed to reduce with seasonal wet-dry cycles as shown in Figure 2b. Figures 3a and 3b present the fluid retentivity and conductivity models respectively.

Table 1. Parameters of Mechanical and Hydraulic Models

Parameter		CH (LL = 80; 44 < PI < 64)	Reference	Selected Parameters
Standard Proctor maximum dry unit weight	$\gamma_{d,max}$ (kN/m^3)	14.8 ± 0.3	Samtani and Nowatzki (2021)	15.1
Standard Proctor optimum moisture content	w_{opt} (%)	25.5 ± 1.2	Samtani and Nowatzki (2021)	24.7
Void ratio	e (-)	0.80 ± 0.04	Samtani and Nowatzki (2021)	0.786
Peak friction angle	ϕ_p' (°)	19 ± 5	Samtani and Nowatzki (2021)	19
Peak cohesion intercept	c_p' (kPa)	11 ± 6	Samtani and Nowatzki (2021)	11
Critical state friction angle	ϕ_{cs}' (°)	19 to 26	Stark et al. (2005)	19
Critical state cohesion intercept	c_{cs}' (kPa)	0	-	0
Residual friction angle	ϕ_r' (°)	9 to 12	Stark et al. (2005)	10
Residual cohesion intercept	c_r' (kPa)	0	-	0
Young's modulus at reference stress 1 atm	E_o (kPa)	230 to 400	Morsy and Helm (2024a) for similar soils	300
Young's modulus stress exponent	m_E (-)	0.25 to 0.35	Morsy and Helm (2024a) for similar CH soils	0.3
Poisson's ratio at reference stress 1 atm	υ_o (-)	0.3	Morsy and Helm (2024a) for similar CH soils	0.3
Poisson's ratio stress exponent	m_υ (-)	0.01 to 0.02	Morsy and Helm (2024a) for similar soils	0.01
Saturated Hydraulic Conductivity	$k_{w,sat}$ (m/s)	$(5 \pm 5) \times 10^{-10}$	Samtani and Nowatzki (2021)	$k_{w,sat} = 1 \times 10^{-8} = \left(\frac{e^5}{1+e}\right)$
Soil-Water Retention Model Fitting Parameter	a_{vg} (-)	0.01 to 0.02	Morsy and Helm (2024a) for similar CH soils	0.23
Soil-Water Retention Model Fitting Parameter	$\psi_{m,o}$ (kPa)		Morsy and Helm (2024a) for similar CH soils	300
Residual Degree of Water Saturation	$S_{w,r}$ (-)	0	Morsy and Helm (2024a) for similar CH soils	0

Figure 2. Shear Strength Model: (a) variation of the angle of internal resistance with deviatoric plastic strain and (b) variation of the cohesion intercept with deviatoric plastic strain. Cohesion intercept peak is allowed to reduce with seasonal wet-dry cycles

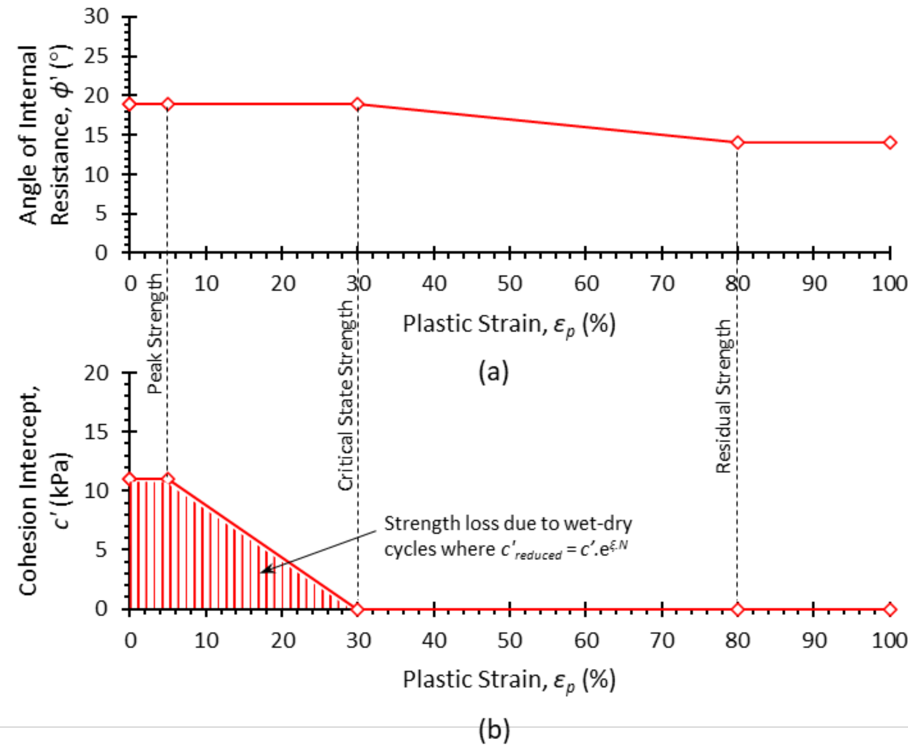

Figure 3. Fluid Models: (a) fluid retentivity models and (b) fluid conductivity models

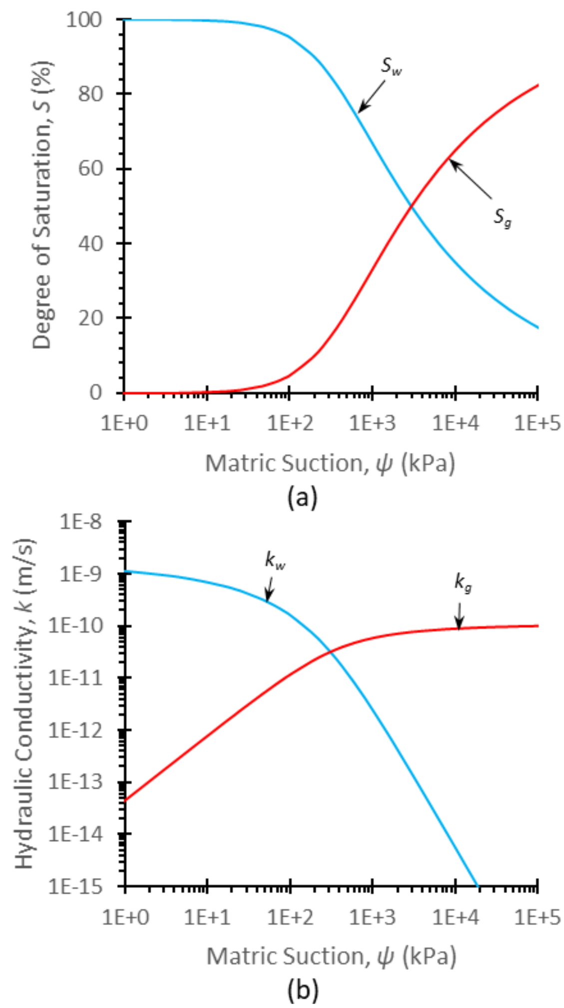

The embankment model geometry was derived from the embankment design specifications and common practice in California. A target side slope would be the desired slope if no right-of-way or foundation constraints were to influence embankment design. A commonly used target side slope is 4H:1V, which the FHWA generally considers a recoverable slope (Beckstrand and Bunn 2024). According to the California Landscape Architecture unit, the recommended target side slope for embankments is 4H:1V. According to the California Geotechnical unit, the recommended maximum side slope is 1.5H:1V. As per the Caltrans Highway Design Manual (Caltrans 2020), embankment end slopes at open end structures should be no steeper than 1.5H:1V for all highways. Accordingly, this study used a side slope of 3H:1V for the emblematic embankment model, which is flatter than 1.5H:1V and slightly steeper than the common target side slope of 4H:1V.

As per the Caltrans Highway Design Manual (Caltrans 2020), embankments shorter than 3 m with side slopes of 2H:1V or flatter may be designed based on past precedence and engineering judgment, provided there are no known problematic soil conditions such as organic soils, soft/loose soils, potentially unstable soils such as Bay Mud or peat, or liquefiable sands. In-depth stability analyses are required for embankments taller than 3 m, embankments with side slope of 2H:1V or steeper, embankments on soft soils, embankments in unstable areas/soils, or embankments constructed from lightweight fills. Accordingly, this study used an embankment height of 6 m, which is twice the limit of embankments that do not require in-depth analysis.

3. Perturbed Climate

Suites of Climate Perturbed Parameter Ensembles (PPEs) were created to effectively mirror the diverse climatic conditions observed in two California districts. A number of climate classifications were considered, including (1) the Köppen climate classification (Figure 4), which is one of the most common global climate classification systems used to denote different climate regions on earth based on local vegetation; (2) the Caltrans pavement climate regions system (Figure 5), which was developed specifically for pavement designs in California and divides the state into climate regions based on the impact of climate on pavements; (3) the CA DWR hydrologic regions system (Figure 6), which classifies regions based on surface water flow and watersheds; and (4) the CIMIS reference evapotranspiration zones system (Figure 7), which was developed to help in urban and agricultural water management planning and water budgeting, as well as designing irrigation systems, planning irrigation schedules, and designing open water evaporation systems.

Figure 4. Köppen Climate Classification of California

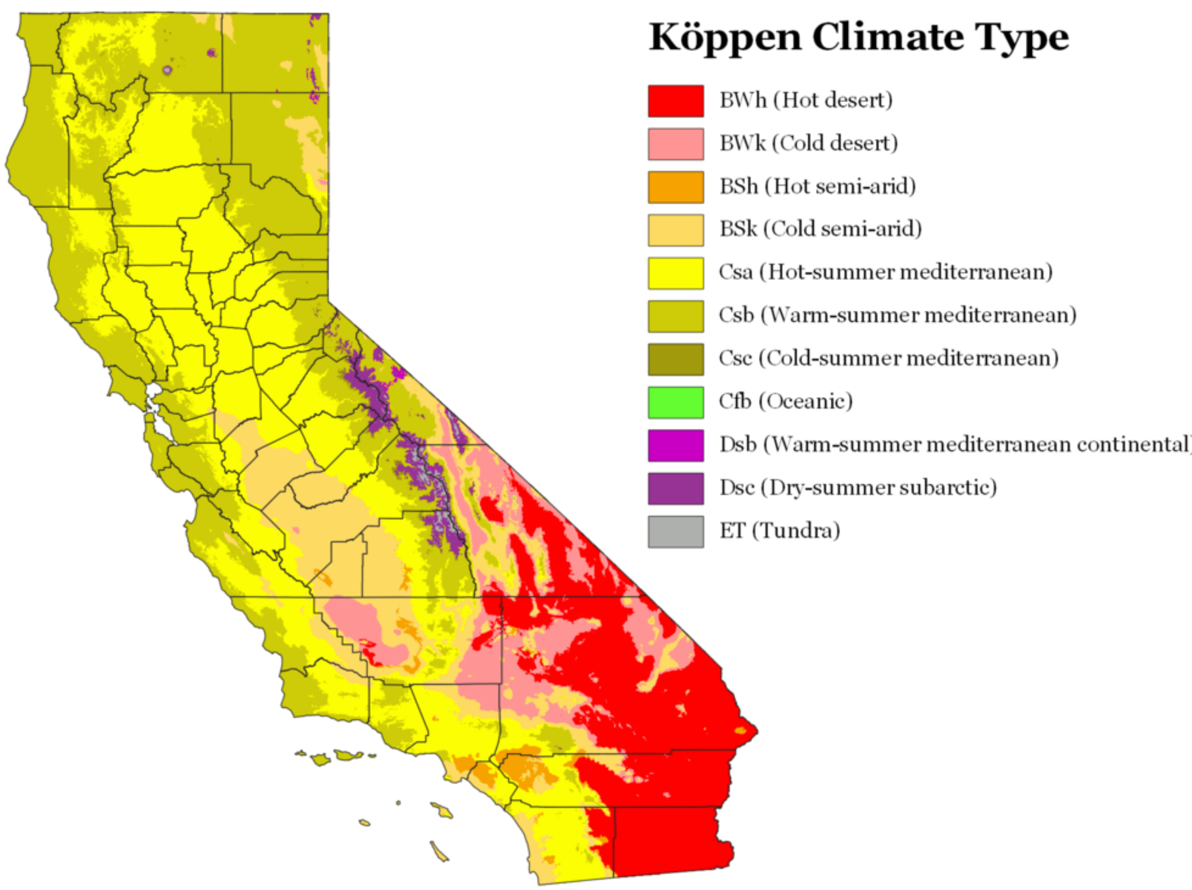

Public domain; 1991–2020 climate normal from PRISM Climate Group, Oregon State University; outline maps from the US Census Bureau.

Figure 5. Caltrans Pavement Climate Regions

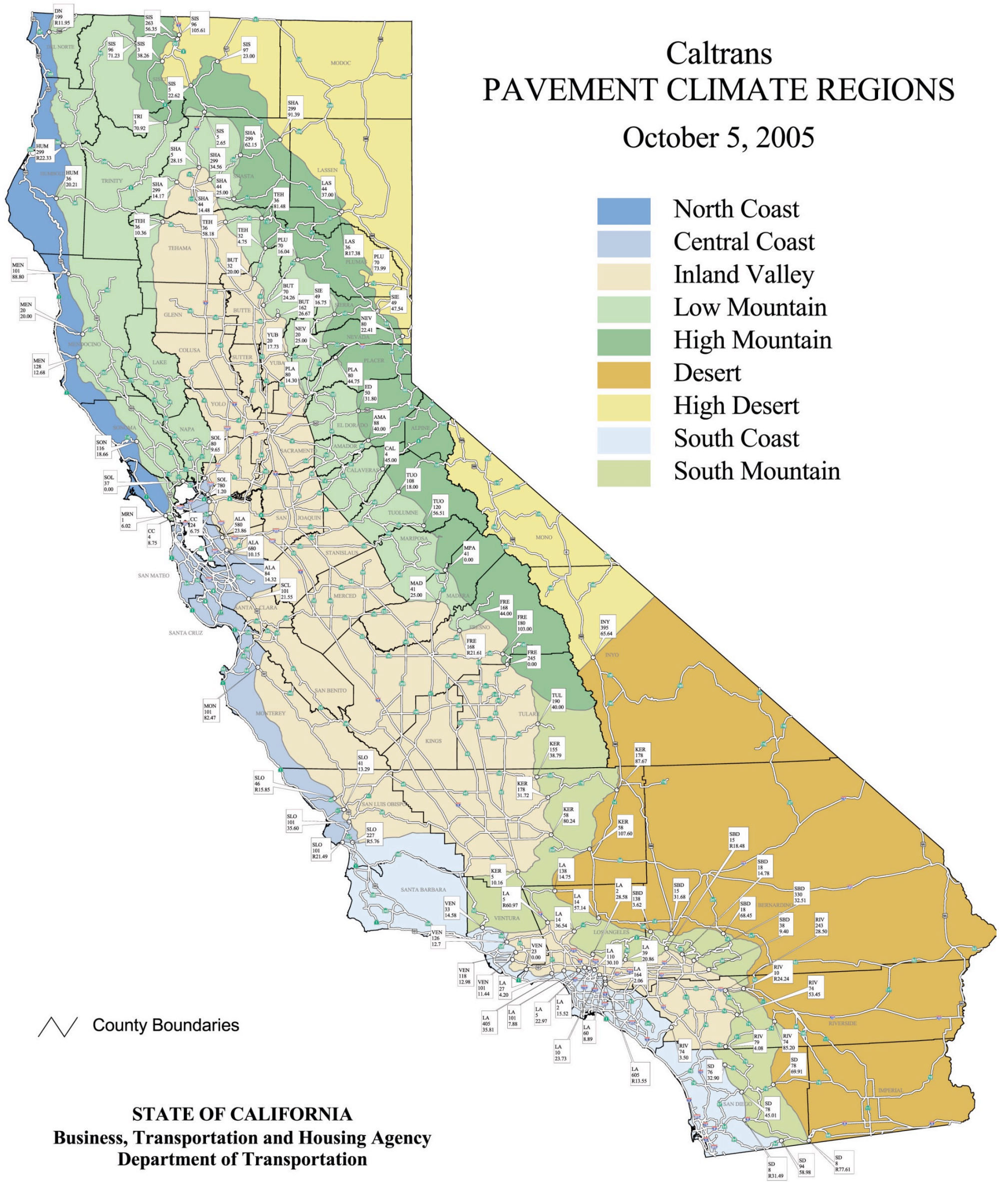

Public domain; Caltrans 2005.

Figure 6. California Hydrologic Regions Map

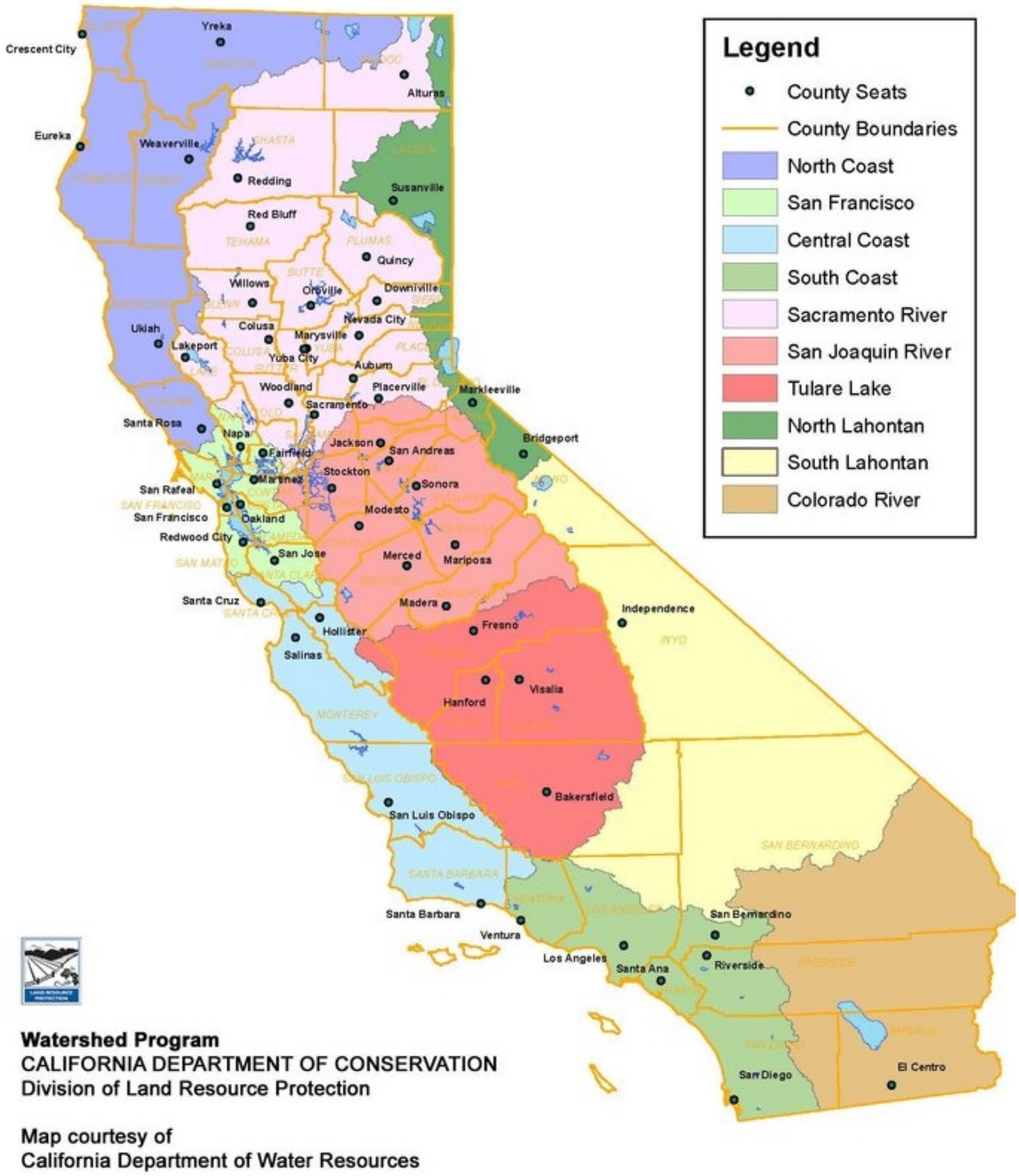

Public domain; California Department of Water Resources.

Figure 7. Reference Evapotranspiration Zones Across California

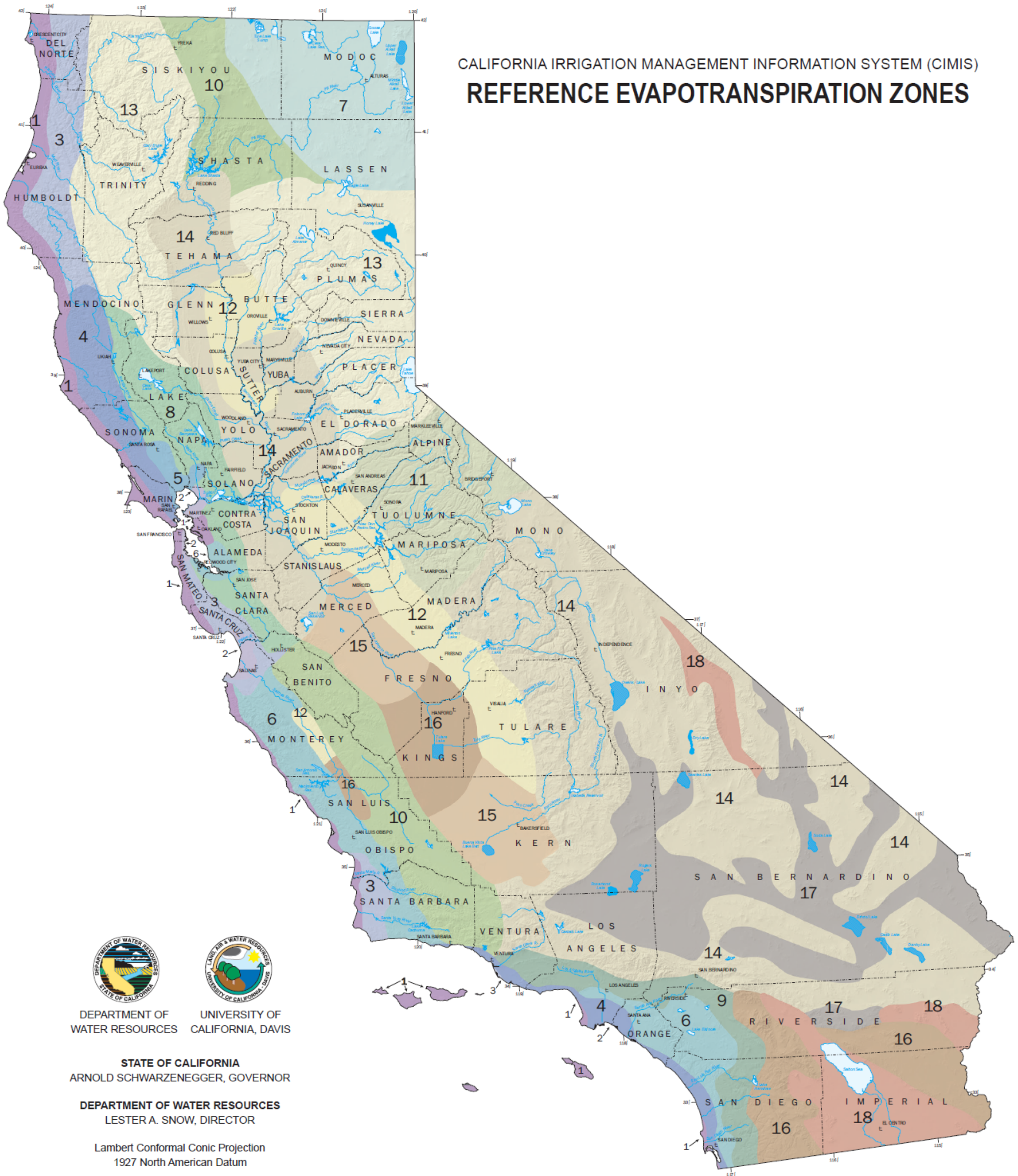

Public domain; California Irrigation Management Information Systems, CIMIS 2012.

3.1 Selection of Study Areas

The selected locations included (i) Los Angeles, which classifies as Warm-Summer Mediterranean (Csb) and is representative of populous coastal areas in Southern California, and (ii) Sacramento, which classifies as Hot-Summer Mediterranean (Csa) and is representative of the populous inland areas in Northern California. Table 2 summarizes the classification of the selected locations using the different classification systems consulted in this study.

Table 2. Summary of the Classification of the Selected Locations Using the Different Classification Systems Consulted in this Study

Classification System	Sacramento, CA	Los Angeles, CA
Köppen climate classification	Hot-Summer Mediterranean (Csa)	Warm-Summer Mediterranean (Csb)
Caltrans pavement climate regions	Inland Valley	South Coast
CA DWR hydrologic regions	Sacramento	South Coast
CIMIS reference evapotranspiration zones	Mid-Central Valley, Southern Sierra Nevada, Tehachapi and High Desert Mountains (High summer sunshine and wind in some locations)	Upland Central Coast and Los Angeles Basin (Higher elevation coastal areas)

3.2 Generation of future weather predictions

According to Najibi and Steinschneider (2023), the weather generator was developed assuming temperature change can be treated by adding step changes to baseline daily maximum and minimum temperature data, which have already been detrended to reflect recent warming, uniformly across the entire spatial domain. They inferred this range of temperature increase from an ensemble of climate model projections selected by the CA DWR Climate Change Technical Advisory Group (CA DWR 2015), which were taken from a subset of ten high-performing GCMs for California from the CMIP5 archive. These projections suggested that +5°C was approximately the maximum amount of warming that could be expected towards the end of the 21st century under the Representative Concentration Pathway (RCP) 8.5 emission scenario (Najibi and Steinschneider 2023).

This study selected four climate scenarios to investigate the effects of changing temperature by +3°C and the precipitation mean by −12.5% and +12.5% on the long-term performance of embankments. Table 3 summarizes the climate scenarios selected for this study. It is notable that these climate scenarios do not include changes in extreme precipitation events.

Table 3. Select Climate Scenarios from Najibi and Steinschneider (2023) Used in Developing Statewide, Weather-Regime Based Stochastic Weather Generator for California

Scenario No.	Incremental Temperature Change (℃)	% Change Extreme Precipitation Quantile	% Change Precipitation Mean
1 (baseline)	0	0	0
25	3	0	-12.5
26	3	0	0
27	3	0	12.5

The Gridded Weather Generator of California, developed by Najibi and Steinschneider (2023) for the California Natural Resources Agency, was used to obtain predicted weather data for this study. The weather generator has two datasets: the past 100-year dataset, and the future 1000-year dataset. Data were downloaded from the past 100-year dataset to compare the weather generator predictions with actual climate data from local weather stations at the locations of the selected sites. Data were downloaded from the future 1000-year dataset for climate scenarios 1, 25, 26, and 27, from which data from 2020 to 2100 were curated for each climate scenario.

Two locations were selected for analysis as discussed earlier: Los Angeles and Sacramento. For Los Angeles, the grid element whose coordinates are 34.03125, -118.15625 was selected because of its relative proximity to the center of the city compared to other adjacent grids. For Sacramento, the grid element whose coordinates are 39.84375, -122.65625 was selected after careful consideration of seven nearby grid elements. These grid elements were ranked based on their proximity to the city center and their distance away from nearby water bodies.

Climate data were used to estimate reference evapotranspiration, ET_0, using the Penman-Monteith method as adopted by FAO56 (Allen et al. 1998) for reference grass, which can be written as follows:

$$ET_0 = \frac{0.408\,\Delta\,(R_n - G) + \gamma\,\frac{900}{T+273}\,u_2(e_s - e_a)}{\Delta + \gamma\,(1 + 0.34\,u_2)} \qquad (7)$$

where R_n is the net radiation at the crop surface in MJ/m²/day; G is the soil heat flux density in MJ/m²/day; T is the mean daily air temperature at 2 m height in °C; u_2 is the wind speed at 2 m height in m/s; e_s is the saturation vapor pressure in kPa; e_a is the actual vapor pressure in kPa; Δ is the slope of vapor pressure curve in kPa/°C; and γ is the psychometric constant in kPa/°C. Refer to Allen et al. (1998) for more details.

The Gridded Weather Generator datasets only offered predictions for the minimum and maximum temperatures and precipitation. To calculate ET_0, additional data and assumptions were required. The solar radiation, R_s, was estimated based on the calculated extraterrestrial radiation, R_a, as follows (Allen et al. 1998):

$$R_s = k_{Rs} R_a \sqrt{(T_{max} - T_{min})} \qquad (8)$$

where T_{max} and T_{min} are the maximum and minimum temperatures in ˚C, and k_{Rs} is an adjustment coefficient that was taken herein as 0.16. The extraterrestrial radiation, R_a , is calculated based on the geographic location and the day of the calendar year, J, as follows:

$$R_a = \frac{1}{\pi} G_{sc}\, d_r\, (\omega_s \sin\varphi \sin\delta + \cos\varphi \cos\delta \sin\omega_s) \qquad (9)$$

where G_{sc} is the solar constant = 0.082 MJ/m^2/min; d_r is the inverse relative distance Earth-Sun and can be calculated as $d_r = 1 + 0.033 \cos\left(\frac{2\pi J}{365}\right)$; ω_s is the sunset hour angle and can be calculated as $\omega_s = \cos^{-1}(-\tan\varphi \tan\delta)$; φ is the latitude; and δ is the solar inclination and can be calculated as $\delta = 0.409 \sin\left(\frac{2\pi J}{365} - 1.39\right)$. Refer to Allen et al. (1998) for more details.

In absence of future relative humidity predictions, the actual vapor pressure, e_a, was estimated based on the dewpoint temperature, T_{dew}, as follows (Allen et al. 1998):

$$e_a = 0.6108 \exp\left(\frac{17.27\, T_{dew}}{237.3 + T_{dew}}\right) \qquad (10)$$

T_{dew} can be estimated in ˚C based on the maximum and minimum temperatures as follows (Linacre 1992):

$$T_{dew} = (0.52) T_{min} + (0.6) T_{max} - (0.009) T_{max}^2 - 2 \qquad (11)$$

Future wind speed data were obtained from the GFDL SPEAR Large Ensembles, which are akin to the California weather generator in that they have a folder for both past data, spanning the years of 1921 to 2014, and future data, spanning the years 2015 to 2100. The past dataset was used and its contents extracted using ArcGIS Pro. Within the software a table of data were generated, listing dates in year-month format alongside corresponding wind speed values. This was then integrated into the curated datasets. Data were downloaded for the same coordinates (i.e., locations) of the selected sites in Los Angeles and Sacramento. Wind speed was assumed to be the same in climate scenarios 1, 25, 26, and 27 studied herein.

To validate the use of the weather generator predictions without any additional climate bias correction, predicted weather parameters from the Gridded Weather Generator were compared to observed historical records. For Los Angeles, historical weather data were obtained from the Los Angeles Downtown weather station located at 34.0678, -118.2417. These observed data were compared to the predictions generated by the model to evaluate its ability to accurately reproduce past conditions, which in turn provides confidence in its capability to predict future weather trends. Figure 8 shows a comparison between the actual and predicted precipitation (Figure 8a) and evapotranspiration (Figure 8b) from 1965 to 2024. It was concluded that the weather generator could reproduce past weather data well and hence is projected to produce reasonable future estimates without bias correction. Similarly, for Sacramento, historical weather data were collected from the Sacramento Airport ASOS weather station situated at 38.50659, -121.49604. This dataset also was used in a similar manner to validate the weather generator's accuracy.

Four climate suites were prepared for each of the selected locations that correspond to climate scenarios 1, 25, 26, and 27. Cumulative precipitation and evapotranspiration of the four suites for Los Angeles and Sacramento are presented in Figures 9 and 10, respectively. Global emissions in Gigatons of Carbon (GtC) for RCP 8.5 (van Vuuren et al. 2011) are plotted in Figures 9 and 10 for reference.

It is notable that the weather data obtained from the weather generator did not show significant shifts in weather patterns or a gradual change in temperature and mean precipitation over time. Instead, the weather generator assumed that the changes in temperature and mean precipitation are constant incremental increases that have taken effect starting in the immediate future.

Figure 8. Comparison Between Actual Weather Data Obtained from Los Angeles Downtown Weather Station and Predicted Weather Data Obtained from the Weather Generator from 1965 to 2024: (a) annual cumulative precipitation and (b) annual cumulative evapotranspiration

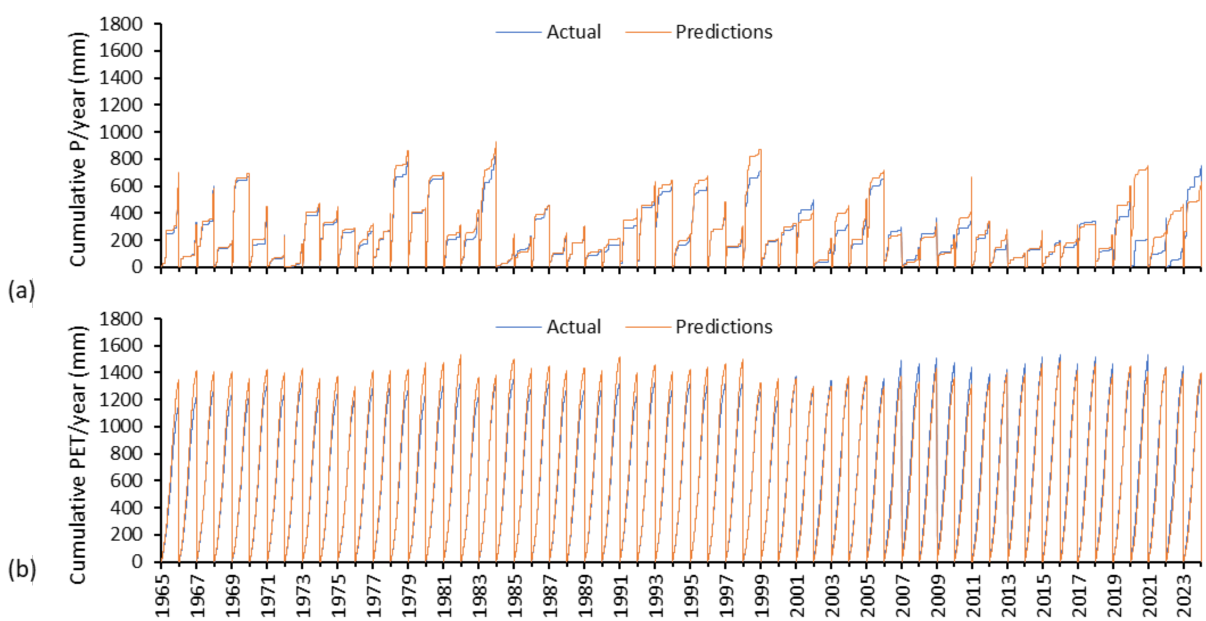

Figure 9. Los Angeles Future Climate Data Predicted Using the Weather Generator for RCP 8.5 Climate Scenarios 1, 25, 26, and 27 from 2020 to 2100: (a) emissions for RCP 8.5 (van Vuuren et al. 2011); (b) cumulative precipitation; and (c) cumulative evapotranspiration

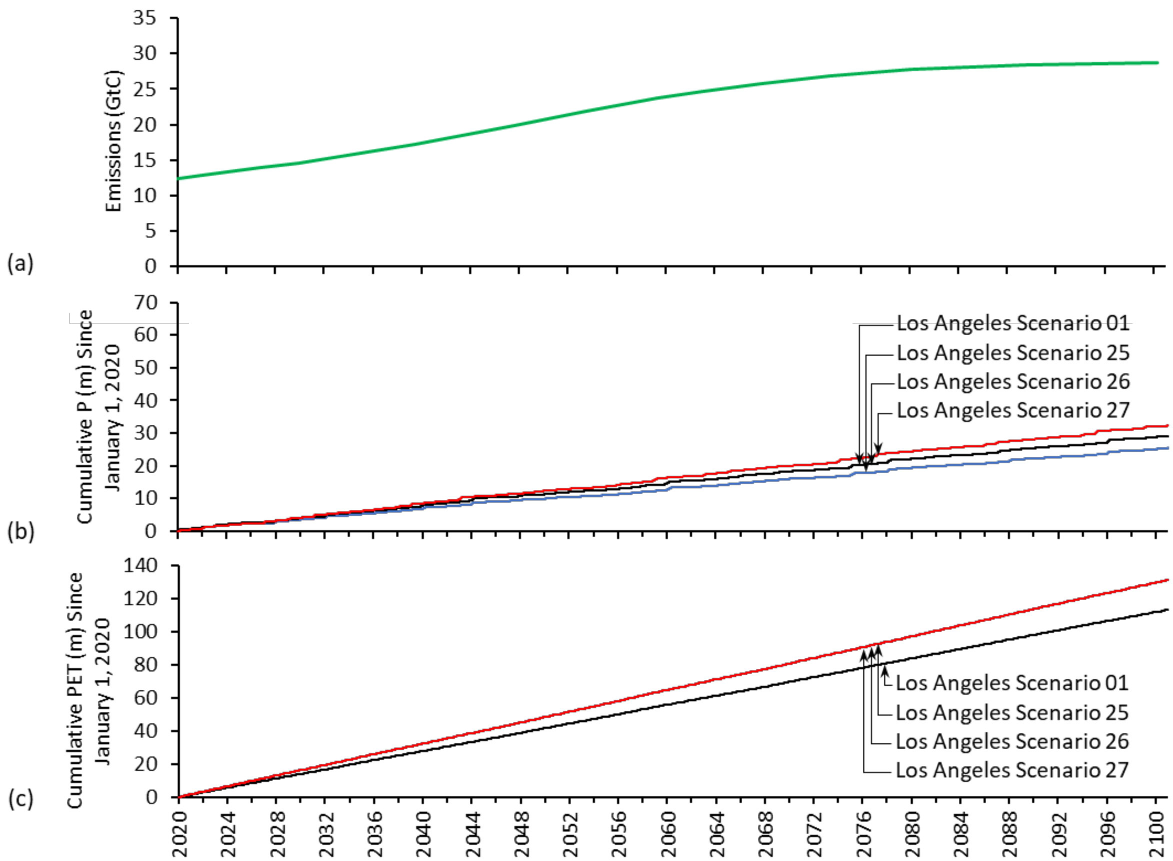

Figure 10. Sacramento Future Climate Data Predicted Using the Weather Generator for RCP 8.5 Climate Scenarios 1, 25, 26, and 27 from 2020 to 2100: (a) emissions for RCP 8.5 (van Vuuren et al. 2011); (b) cumulative precipitation; and (c) cumulative evapotranspiration

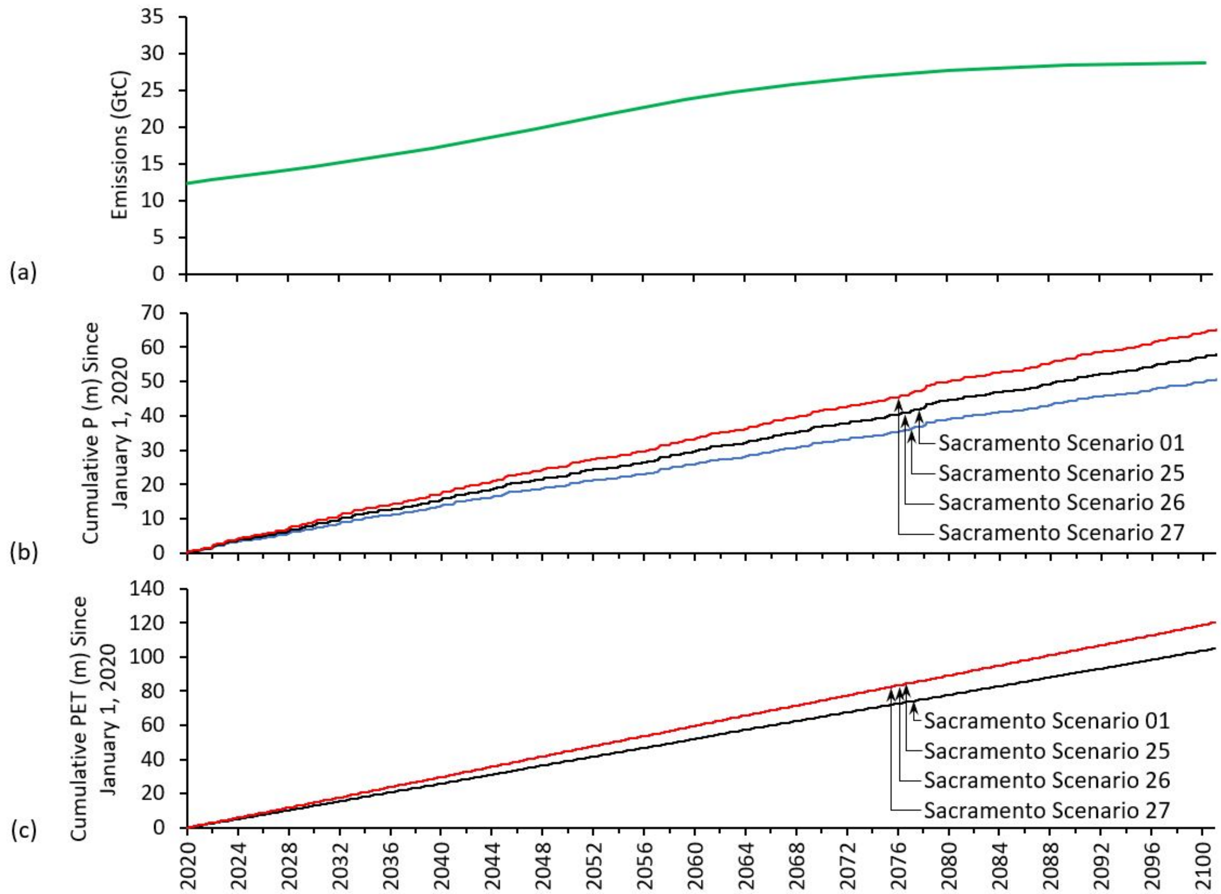

3.3 Climate incorporation in Numerical Model

A transient climate boundary was defined at the surface of the model to simulate soil-atmosphere interaction. The climate boundary calculates the daily surface available net flux as the difference between precipitation and evapotranspiration in each simulation day. The daily available net flux values were divided uniformly over 24 hours and input in the climate boundary subroutine at every surface mesh node as it executed every one simulation hour to determine a boundary flux based on each node's pore pressure and saturation condition, as shown in Figure 11. A detailed description is available in Morsy et al. (2023a).

Figure 11. Ground Surface Moisture Flux

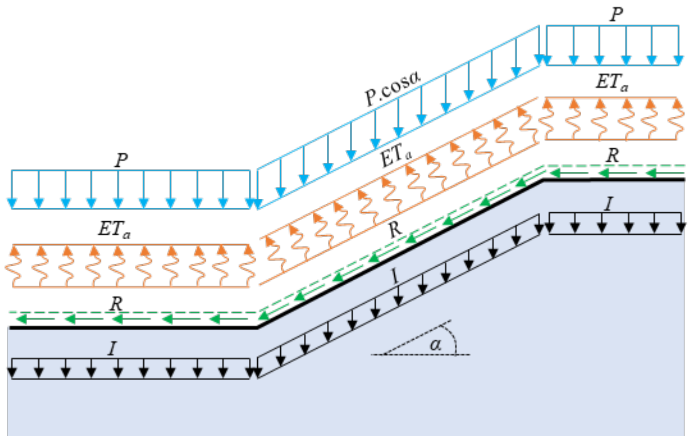

Adapted from Fredlund et al. 2012.

4. Parametric Study

The parametric evaluation focused on studying the long-term performance of an emblematic embankment under various climate conditions at two climate locations in California: Los Angeles and Sacramento. To facilitate the discussion, the Los Angeles simulations under climate scenarios 1, 25, 26, and 27 were given IDs LOS01, LOS25, LOS26, and LOS27; similarly, Sacramento simulations under climate scenarios 1, 25, 26, and 27 were given IDs SAC01, SAC25, SAC 26, and SAC 27. It is notable that the time histories of all models under the various climate scenarios follow the same trend with different magnitudes. This is an artefact of the future California climate predictions (precipitation and temperature) which varied by constant increments, as discussed earlier.

Figures 12a and 12b present the time histories of the predicted mid-slope matric suction at a depth of 1 m for Los Angeles and Sacramento simulations, respectively. Each subfigure presents the matric suction variation corresponding to the four climate scenarios considered in this study (scenarios 1, 25, 26, and 27).

When comparing the numerical predictions of LOS01 and LOS26, it was observed that the increase in future temperature by +3°C without a change in future mean precipitation will result in an overall slightly drier slope as indicated by the higher near-surface matric suction observed in LOS26 compared to LOS01. An approximately 9% increase was observed in the predicted near-surface matric suction under climate scenario 26 compared to climate scenario 1.

When comparing the numerical predictions of LOS25, LOS26, and LOS27, it was observed that the near-surface matric suction is likely to decrease (wetter slopes) with increasing the change in future mean precipitation. The difference in predicted matric suction between LOS27 (+12.5% change in mean precipitation) and LOS25 (–12.5% change in mean precipitation) was approximately –15%. The difference in predicted matric suction between LOS27 (+12.5% change in mean precipitation) and LOS26 (0% change in mean precipitation) was approximately –6%.

When comparing the numerical predictions of Los Angeles simulations to Sacramento simulations, it was observed that the Los Angeles models were generally drier with scattered wet years separated by prolonged dry periods (see Figure 12a). Nevertheless, Sacramento models exhibited consistent seasonal cycles of wetting and drying (see Figure 12b). This is attributed to the wetter climate of Sacramento in comparison to Los Angeles (see Figures 9 and 10).

Figure 12. Predicted Time Histories of Mid-Slope Matric Suction at Depth 1 M from the Slope Surface for Climate Scenarios 1, 25, 26, and 27: (a) for Los Angeles simulations and (b) for Sacramento simulations

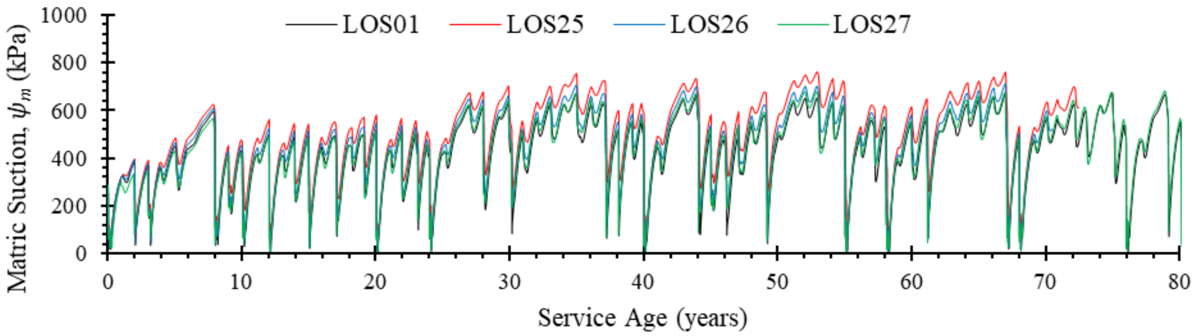

(a)

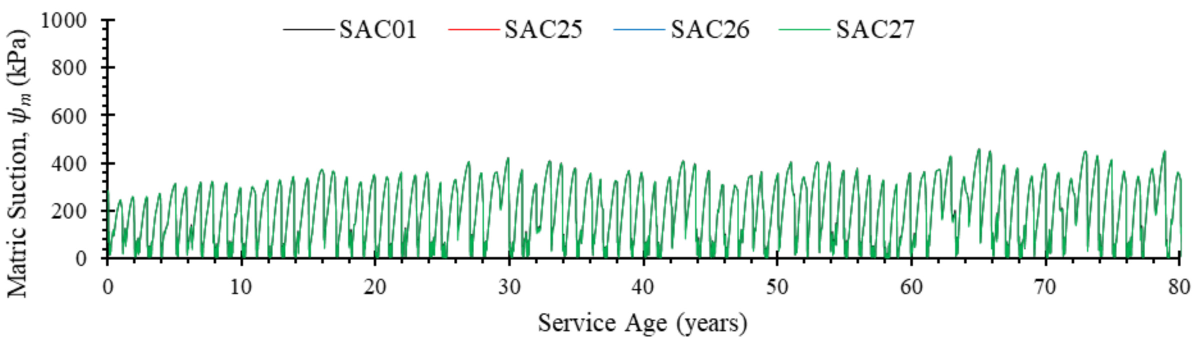

(b)

Figures 13a and 13b present the time histories of the predicted mid-slope outward displacement at the slope surface for Los Angeles and Sacramento simulations respectively. Each subfigure presents the cumulative outward displacement over time corresponding to the four climate scenarios considered in this study (scenarios 1, 25, 26, and 27). It is notable that the numerical model was able to capture the seasonal variation in outward displacements. During every wet season, an outward displacement takes place, part of which recovers during the subsequent dry season. After every wet-dry cycle, an irrecoverable displacement (permanent deformation) will accumulate over time. Like the time histories in Figure 12, the time histories in Figure 13 of all models under the various climate scenarios follow the same trend with different magnitudes.

When comparing the numerical predictions of LOS01 and LOS26, it was observed that the increase in future temperature by +3°C without a change in future mean precipitation will result in an overall slightly less outward displacement. This is attributed to the drier slopes (with higher matric suction and effective stress) under elevated future temperature and no change in mean precipitation, as discussed earlier. An approximately 15% decrease was observed in the predicted mid-slope outward displacement under climate scenario 26 in comparison to climate scenario 1.

When comparing the numerical predictions of LOS25, LOS26, and LOS27, it was observed that the mid-slope outward displacement is likely to increase with increasing the change in future mean precipitation, especially later in the service life as irrecoverable outward displacements accumulate. The difference in predicted mid-slope outward displacement between LOS27 simulation (+12.5% change in mean precipitation) and LOS25 (–12.5% change in mean precipitation) is approximately +31%. The difference in predicted mid-slope outward displacement between LOS27 simulation (+12.5% change in mean precipitation) and LOS26 (0% change in mean precipitation) is approximately +26%.

When comparing the numerical predictions of Los Angeles simulations to Sacramento simulations, it was observed that the mid-slope outward displacement predicted in the Sacramento models was much higher than the Los Angeles models. This is attributed to the wetter climate of Sacramento in comparison to Los Angeles, which leads to less matric suction (and effective stress) in the embankment near-surface zones.

Figure 13. Predicted Time Histories of Mid-Slope Outward Displacement at the Slope Surface for Climate Scenarios 1, 25, 26, and 27: (a) for Los Angeles simulations and (b) for Sacramento simulations

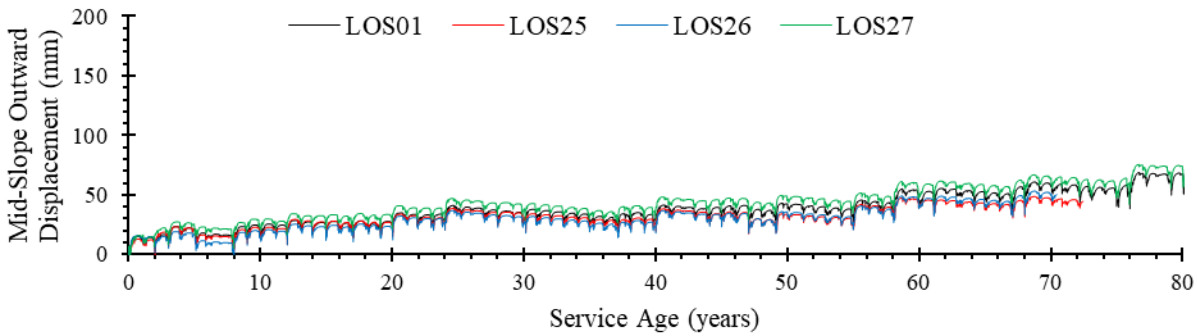

(a)

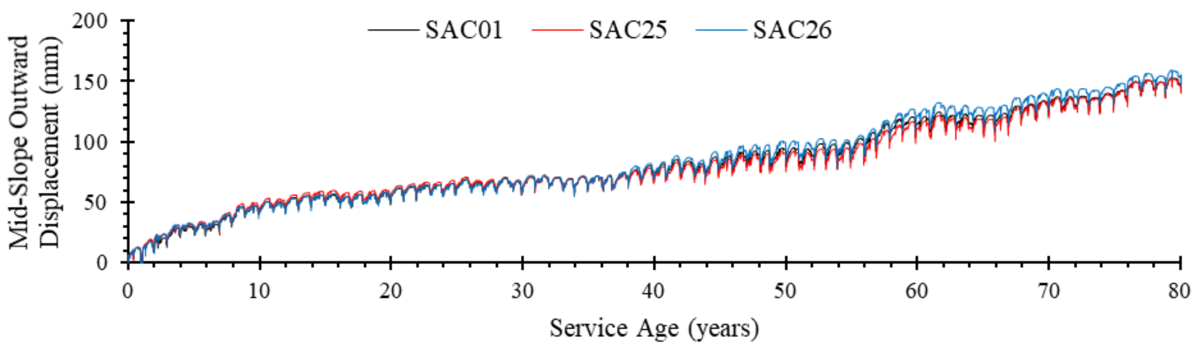

(b)

Figures 14a and 14b present the time histories of the predicted mid-slope vertical displacement at the slope surface for Los Angeles and Sacramento simulations respectively. Each subfigure presents the cumulative vertical displacement over time corresponding to the four climate scenarios considered in this study (scenarios 1, 25, 26, and 27). Like outward displacements, the numerical model was able to capture the seasonal variation in vertical displacements. During every wet season, a vertical displacement (swelling) takes place, part of which recovers during the subsequent dry season (shrinkage). After every wet-dry cycle, an irrecoverable swelling (permanent deformation) will accumulate over time. Again, like the time histories in Figures 12 and 13, the time histories in Figure 14 of all models under the various climate scenarios follow the same trend with different magnitudes.

When comparing the numerical predictions of LOS01 and LOS26, it was observed that the increase in future temperature by +3°C without a change in future mean precipitation will result in an insignificant difference in vertical displacement.

When comparing the numerical predictions of LOS25, LOS26, and LOS27, it was observed that the mid-slope vertical displacement is likely to decrease with increasing the change in future mean precipitation, especially later in the service life as irrecoverable vertical displacements accumulate. The difference in predicted vertical displacement between LOS27 simulation (+12.5% change in mean precipitation) and LOS25 (–12.5% change in mean precipitation) was approximately +13%. The difference in predicted vertical displacement between LOS27 simulation (+12.5% change in mean precipitation) and LOS26 (0% change in mean precipitation) was approximately +7%.

When comparing the numerical predictions of Los Angeles simulations to Sacramento simulations, it was observed that the mid-slope vertical displacement predicted in the Sacramento models was much higher than that predicted in the Los Angeles models. This is attributed to the wetter climate of Sacramento in comparison to Los Angeles, which leads to larger swelling in the embankment near-surface zones.

Figure 14. Predicted Time Histories of Mid-Slope Vertical Displacement at the Slope Surface for Climate Scenarios 1, 25, 26, and 27: (a) for Los Angeles simulations and (b) for Sacramento simulations

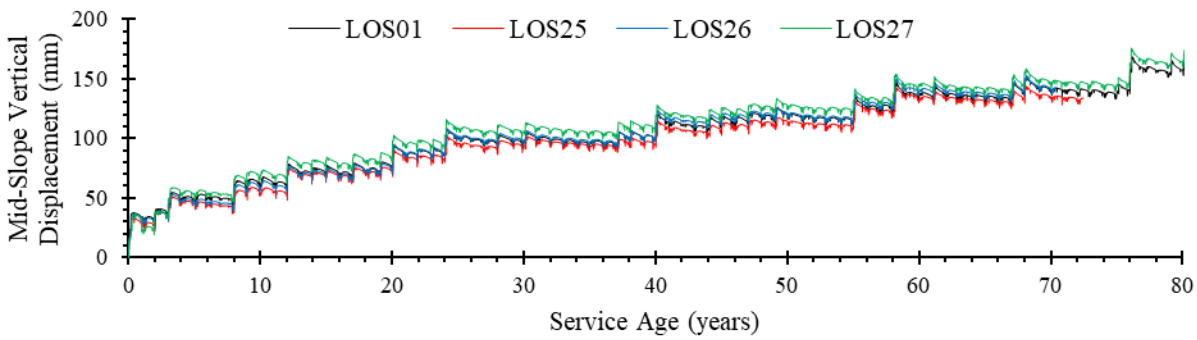

(a)

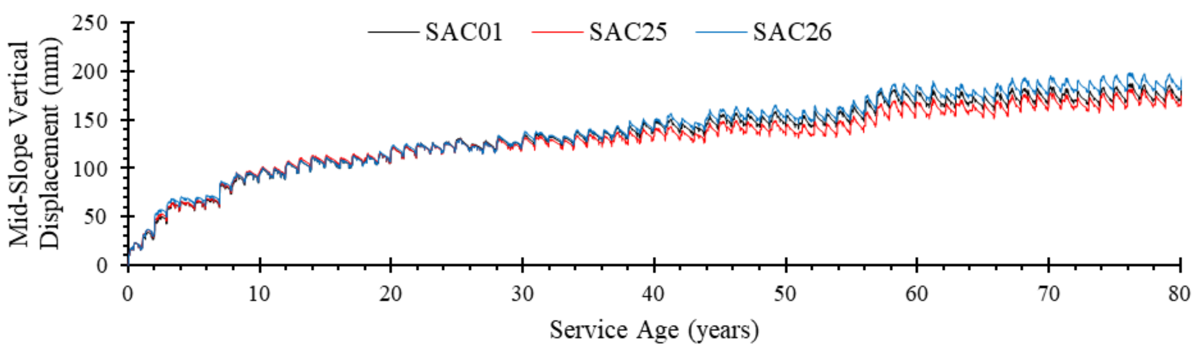

(b)

Figures 15a and 15b present the mid-slope vertical displacement versus outward displacement at the slope surface for LOS01 and SAC01 simulations respectively. These figures provide the trajectory of the slope surface over time. As shown in the figures, the predictions show an "oscillatory" displacement of the slope surface with seasonal cycles of wetting and drying. It was observed that the rate of increase in irrecoverable vertical displacement decreases after some level that could be correlated to the soil swelling potential, whereas the increase in irrecoverable outward displacement persists.

Figure 15. Predicted Mid-Slope Vertical Displacement Versus Outward Displacement at the Slope Surface: (a) for Los Angeles simulation under climate scenario 1 and (b) for Sacramento simulation under climate scenario 1

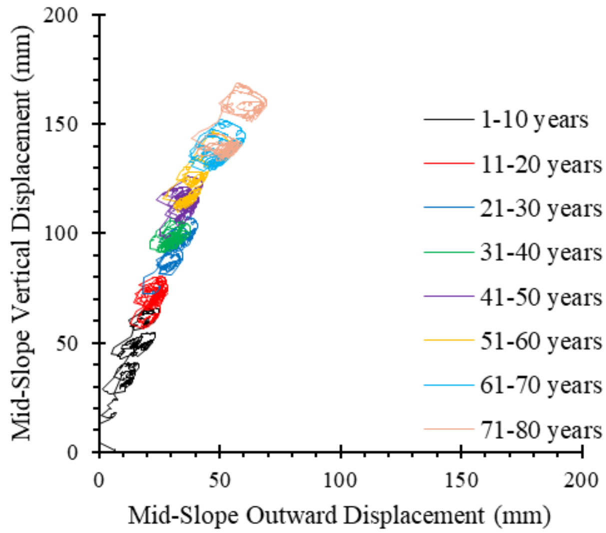

(a)

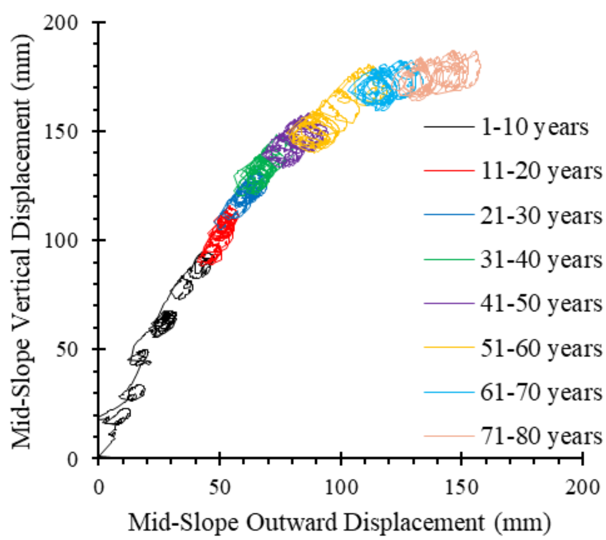

(b)

Long-term performance predictions for embankments other than the emblematic embankment studied herein, or for those constructed in climate types other than those studied herein, can be obtained by running additional simulations using the numerical model presented in this study. Tentatively, the long-term performance of embankments comparable to the emblematic embankment studied herein and in other climate zones may be approximated by adjusting the results predicted at the exemplar locations studied herein using relevant climate zone characteristic parameters, such as the ratio of the average annual potential evapotranspiration to the average annual precipitation (PET/P). Figure 16 shows correlations between the average surface displacement rate (vertical and outward) and the ratio of average potential evapotranspiration to average precipitation for the simulations conducted in this study. Other relevant climate zone characteristic parameters that consider the soil type include the Thornthwaite Moisture Index (TMI). However, further investigation is required to test the validity of this hypothesis.

Figure 16. Correlation Between the Average Surface Displacement Rate with the Ratio of Average Potential Evapotranspiration to Average Precipitation

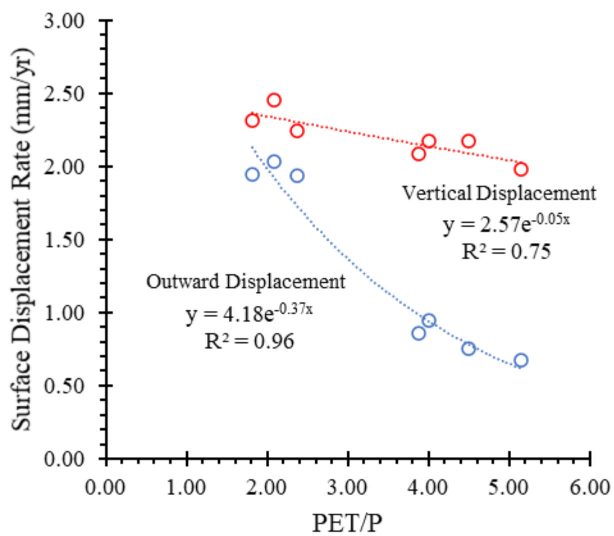

5. Summary and Recommendations

Embankments are key transportation infrastructure features providing essential support for long, linear stretches of transportation infrastructure, including highways and railways, in California and globally. Clay embankments are susceptible to weather-related deterioration processes that can gradually compromise their stability and, in some cases, lead to unexpected failures. Climate change, along with the associated shifts in weather patterns, is projected to adversely impact the weather-related deterioration processes leading to exacerbated failures and/or shorter service life. This study evaluated the impact of climate change on the rate of weather-driven deterioration of embankments in two locations in California: Los Angeles and Sacramento. Specifically, a multi-phase hydromechanical geotechnical model was developed for an exemplar clay embankment. The model is capable of simulating long-term performance of an embankment subject to a climate-controlled flux boundary. The model was used to perform numerical simulations with various climate perturbed parameter ensembles of four future climate scenarios:

- Case (1) no average temperature or average precipitation changes.
- Case (2) +3°C average temperature change and –12.5% average precipitation change.
- Case (3) +3°C average temperature change and no average precipitation change.
- Case (4) +3°C average temperature change and +12.5% average precipitation change.

Performance indicators were obtained from the numerical simulations to compare the effects of climate change in Los Angeles and Sacramento. Overall, it was concluded that climate change is generally projected to adversely affect the long-term performance of clay embankments. The following insights can be drawn from the study:

- The increase in future temperature by +3°C without a change in future mean precipitation is likely to lead to drier slopes and higher matric suction. An approximately 9% increase was observed in the predicted near-surface matric suction as a result of +3°C incremental change in future temperature and no change in future mean precipitation.
- The increase in future mean precipitation is likely to lead to wetter slopes and lower matric suction. An approximately 6% decrease was observed in the predicted near-surface matric suction as a result of a +12.5% incremental change in mean precipitation and excluding the effect of a +3°C incremental change in future temperature.
- The increase in future temperature by +3°C without a change in future mean precipitation is likely to lead to smaller outward slope displacements and insignificant changes in vertical displacements. An approximately 15% decrease was observed in the predicted mid-slope

outward displacements as a result of a +3°C incremental change in future temperature and no change in future mean precipitation.

- The increase in future mean precipitation is likely to lead to larger outward and vertical slope displacements. An approximately 26% increase was observed in the predicted mid-slope outward slope displacements and an approximately 7% increase was observed in vertical slope displacements as a result of a +12.5% incremental change in mean precipitation and excluding the effect of a +3°C incremental change in future temperature.

- The predicted trajectory of the slope surface over time showed an "oscillatory" displacement of the slope surface with seasonal cycles of wetting and drying. Slope displacements increase during the wet seasons and partially rebound during the dry seasons. The net cumulative displacements (irrecoverable displacements) are outwards and upwards, which increase over time as the slope experiences more cycles of wetting and drying.

- The rate of increase in irrecoverable vertical displacements was observed to decrease after reaching some swelling level, which could be correlated to the soil swelling potential, whereas the increase in irrecoverable outward displacement persists. Swelling-induced shallow slides are likely triggered at this condition. This is likely to occur in high plasticity clays, such as the clay used in the emblematic embankment herein, after 65 years in the Los Angeles climate and after 40 years in the Sacramento climate. Existing embankments constructed from high plasticity clays that are older than these limits and whose failure consequences are high may require risk mitigation strategies (e.g., monitoring).

- Long-term performance prediction for embankments other than the emblematic embankment studied herein, or those constructed in climate types other than those studied herein, can be obtained by running additional simulations using the numerical model presented in this study. Tentatively, the long-term performance of embankments comparable to the emblematic embankment studied herein and in other climate zones may be approximated by adjusting the results predicted at the exemplar locations studied herein using relevant climate zone characteristic parameters, such as the ratio of the average annual potential evapotranspiration to the average annual precipitation (PET/P).

Bibliography

Allen, R.G., Pereira, L.S., Raes, D., and Smith, M. (1998). *Crop evapotranspiration-Guidelines for computing crop water requirements-FAO Irrigation and drainage paper 56*. FAO, Rome, 300(9), D05109.

Beckstrand, D., and Bunn, M. (2024). *Prevention and Mitigation of Surficial Slope Failures on Fill Highway Embankment Slopes*. NCHRP Synthesis 617, National Academies of Sciences, Engineering, and Medicine (NASEM), Washington, DC: The National Academies Press. https://doi.org/10.17226/27645.

Bedsworth, L., Cayan, D., Franco, G., Fisher, L., and Ziaja, S. (2018). California's Fourth Climate Change Assessment. *Statewide Summary Report. California Governor's Office of Planning and Research. Scripps Institution of Oceanography. California Energy Commission. California Public Utilities Commission*.

Bishop, A. W. (1959). "The principle of effective stress." *Teknisk ukeblad,* Vol. 39, pp. 859–863.

Caltrans (2005). *Caltrans Pavement Climate Regions Map*. California Department of Transportation (Caltrans), October 2005.

Caltrans (2018). *Caltrans Climate Change Vulnerability Assessment Summary Report*. California Department of Transportation.

Caltrans (2020). *Highway Design Manual*. Seventh Edition, California Department of Transportation, Sacramento, CA.

CA DWR (2024). California Groundwater Live. California Department of Water Resources (CA DWR) https://sgma.water.ca.gov/CalGWLive/ (accessed on 13 June 2024).

CA DWR (2015). Gridded Weather Generator Perturbations of Historical Detrended and Stochastically Generated Temperature and Precipitation for the State of CA and HUC8s. https://data.ca.gov/dataset/gridded-weather-generator-perturbations-of-historical-detrended-and-stochastically-generated-te (accessed on 15 January 2024).

CIMIS (2012). *Reference Evapotranspiration Zones*, California Irrigation Management Information System (CIMIS), California Department of Water Resources (CA DWR), January 2012, 4p.

Fredlund, D.G., Rahardjo, H., and Fredlund, M.D. (2012). *Unsaturated Soil Mechanics in Engineering Practice.* John Wiley & Sons, Inc.

Helm, P.R., Svalova, A., Morsy, A.M., Rouainia, M., Smith, A., El-Hamalawi, A., Wilkinson, D., Postill, H., and Glendinning, S. (2024), "Emulating Long-Term Weather-Driven Transportation Earthworks Deterioration Models to Support Asset Management," *Transportation Geotechnics*, *44*.

Itasca (2019). *Fast Lagrangian Analysis of Continua V. 8.1 – User's Guide*. 1st edition, Itasca Consulting Group Inc., Minneapolis, US.

Kovacevic, N., Hight, D.W., Potts, D.M., and Carter, I.C. (2013). "Finite-element analysis of the failure and reconstruction of the main dam embankment at Abberton Reservoir, Essex, UK." *Geotechnique*, *63*, 753–767.

Kulhawy, F.H., Duncan, J.M., and Seed, H.B. (1969). *Finite element analyses of stresses and movements in embankments during construction*. U.S. Army Engineer Waterways Experiment Station, Vicksburg, Mississippi, US.

Linacre, E. (1992). *Climate data and resources: A reference and guide*. Psychology Press.

Masson-Delmotte, V. P., Zhai, P., Pirani, S. L., Connors, C., Péan, S., Berger, N., ... & Scheel Monteiro, P. M. (2021). IPCC 2021: *Summary for policymakers. in: Climate change 2021: The physical science basis*. Contribution of Working Group I to the Sixth Assessment Report of the Intergovernmental Panel on Climate Change (IPCC).

Morsy, A. M. (2024). *Time-To-Failure Prediction of Fine-Grained Soil Slopes Subject to Weather-Driven Deterioration*, Report No. 24-20, Mineta Transportation Institute (MTI), San Jose, CA. https://doi.org/10.31979/mti.2024.2326

Morsy, A. M., and Helm, P. R. (2024a), "Failure Prediction of Clay Embankments Subject to Weather-Driven Deterioration," *Journal of Geotechnical and Geoenvironmental Engineering*, *150*(12).

Morsy, A. M., and Helm, P. R. (2024b). *Meteorological Data Used for Water-Balance Calculations at Ground Surface in Failure Prediction of Clay Embankments Subject to Weather-Driven Deterioration*. Dataset, Newcastle University. https://doi.org/10.25405/data.ncl.26349286

Morsy, A.M., Helm, P.R., El-Hamalawi, A., Smith, A., Hughes, P.N., Stirling, R.A., Dijkstra, T.A., Dixon, N., and Glendinning, S. (2023a), "Development of a Multi-Phase Numerical Modeling Approach for Hydromechanical Behavior of Clay Embankments Subject to Weather-Driven Deterioration," *Journal of Geotechnical and Geoenvironmental Engineering*, *149*(8).

Morsy, A.M., Helm, P.R., El-Hamalawi, A., Smith, A., Hughes, P.N., Stirling, R.A., Dijkstra, T.A., Dixon, N., and Glendinning, S. (2023b). *Data Used for the Validation of the BIONICS Research Embankment Hydromechanical Model*. Dataset, Newcastle University. https://doi/org/10.25405/data.ncl.22144442

Mualem, Y. (1976). "A new model for predicting the hydraulic conductivity of unsaturated porous media." *Water Resources Research*, Vol. 12, No. 3, pp. 513–522.

Najibi, N., and Steinschneider, S. (2023). *A process-based approach to bottom-up climate risk assessments: developing a statewide, weather-regime based stochastic weather generator for California*, Final Report. California Department of Water Resources (CA DWR), August 2023, 67p.

Nyambayo, V. P., and Potts, D. M. (2010). "Numerical simulation of evapotranspiration using a root water uptake model." *Computers and Geotechnics*, *37*(1-2), 175–186.

Nyambayo, V.P., Potts, D.M., and Addenbrooke, T.I. (2004). "The influence of permeability on the stability of embankments experiencing seasonal cyclic pore water pressure changes." In *Proceedings of Advances in Geotechnical Engineering: The Skempton Conference*, 898–910.

Postill, H., Helm, P. R., Dixon, N., Glendinning, S., Smethurst, J. A., Rouainia, M., Briggs, K.M., El-Hamalawi, A., and Blake, A.P. (2021). "Forecasting the long-term deterioration of a cut slope in high-plasticity clay using a numerical model." *Engineering Geology*, *280*, 105912.

Potts, D.M., and Zdravkovic, L. (1999). *Finite element analysis in geotechnical engineering: Theory.* Thomas Telford.

Rouainia, M., Davies, O., O'Brien, T., and Glendinning, S. (2009). "Numerical modelling of climate effects on slope stability." *Proceedings of the Institution of Civil Engineers-Engineering Sustainability*, *162*, 81–89.

Samarasinghe, A.M., Huang, Y.H., and Drnevich, V.P. (1982). "Permeability and consolidation of normally consolidated soils." *Journal of the Geotechnical Engineering Division*, *108*(6), 835–850.

Samtani, N.C., and Nowatzki, E.A. (2021). *Mechanically Stabilized Earth (MSE) Wall Fills—A Framework for Use of Local Available Sustainable Resources (LASR)*. Report No. FHWA-HIN-21-002. Federal Highway Administration (FHWA): Washington, DC, US.

Stark, T.D., Choi, H., and McCone, S. (2005). "Drained shear strength parameters for analysis of landslides." *Journal of Geotechnical and Geoenvironmental Engineering*, *131*(5), 575–588.

Stirling, R.A., Toll, D.G., Glendinning, S., Helm, P.R., Yildiz, A., Hughes, P.N., and Asquith, J.D. (2021). "Weather-driven deterioration processes affecting the performance of embankment slopes." *Géotechnique*, *71*(11), 957–969.

TAMP (2022). *California transportation asset management plan*. California Department of Transportation (Caltrans).

Templeton, A.E., Sills, G.L., and Cooley, L.A. (1984). "Long term failure in compacted clay slopes." In *Proceedings of International Conference on Case Histories in Geotechnical Engineering*, 749–754.

van Genuchten, M.T. (1980). "A closed - form equation for predicting the hydraulic conductivity of unsaturated soils." *Soil Science Society of America Journal*, *44*(5), 892–898.

van Vuuren, D. P., Edmonds, J., Kainuma, M., Riahi, K., Thomson, A., Hibbard, K., ... & Rose, S. K. (2011). The representative concentration pathways: An overview. *Climatic Change*, *109*, 5–31.

Vaughan, P.R., Kovacevic, N., and Potts, D.M. (2004). "Then and now: some comments on the design and analysis of slopes and embankments." In *Proceedings of Advances in Geotechnical Engineering: The Skempton Conference*, 241–290.

About the Authors

Amr M. Morsy, PhD, PE

Dr. Amr Morsy is a professional civil engineer with experience in both academia and industry. His research focuses on geotechnical engineering, transportation geotechnics, environmental geotechnics, and climate adaptation. He obtained his B.Eng and M.Sc. degrees in civil engineering from Cairo University in 2011 and 2013 respectively and obtained his PhD degree in civil engineering from The University of Texas at Austin in 2017. He worked as a postdoctoral fellow at The University of Texas at Austin in 2018 and as a practicing geotechnical engineer from 2018 to 2020. He later worked as a research associate at Loughborough University on the ACHILLES program grant from 2020 to 2022. He has been working as an assistant professor at California State University, Long Beach since 2022.

As part of his academic experience, Dr. Morsy conducts research on geotechnical infrastructure deterioration and asset management, climate change impacts on geotechnical infrastructure, and geotechnical solutions for sustainable built environments. He has excelled in physical and numerical modeling of geotechnical and geoenvironmental engineering systems, and in infrastructure instrumentation and laboratory experimentation. He participated in research projects sponsored by the Transportation Research Board of the National Academies of Sciences, Engineering, and Medicine, the Engineering and Physical Sciences Research Council of the UK Research and Innovation, the US Federal Highway Administration, the Geosynthetic Institute, and the Departments of Transportation of Texas and Indiana.

As part of his professional consulting experience, Dr. Morsy conducts rigorous analyses, designs, and forensic evaluations for a range of slopes, retaining walls, reinforced soil structures, deep excavations, bridge foundations, waste containment facilities, tailings dams, and embankment dams. He assisted expert witnesses in cases involving collapse and poor performance of earth retaining structures. He provided solutions to geotechnical problems in a number of environmental remediation projects involving cleanup of superfund sites. He conducted multi-phase flow analyses for several infrastructure features including earthworks, embankment dams, and cover systems. Some of the consulting projects he participated in served the US Environmental Protection Agency, New York State Department of Environmental Conservation, New York State and Indiana Departments of Transportation, Tennessee Valley Authority, New Jersey Transit, and several multinational private and public corporates.

Emma Varela

Emma Varela is a physics major in her junior year at California State University, Long Beach with a passion for the discipline and its interdisciplinary applications. Emma's academic and research experiences have allowed her to explore the intersection of physics with other fields, such as engineering and climatology, while developing technical expertise and problem-solving skills. The research she is currently contributing to utilizes climate simulations to evaluate the deterioration of earthworks, with its ultimate aim being to develop innovative solutions with lasting impacts.